Journal of Power Sources 241 (2013) 281–287

Contents lists available at SciVerse ScienceDirect

Journal of Power Sources

journal homepage: www.elsevier.com/locate/jpowsour

Short communication

On the interaction of SSC and LSGM in composite SOFC electrodes

Anh T. Duong [a,b], Daniel R. Mumm [a,b,*]

[a] Chemical Engineering and Materials Science, University of California, Irvine, CA 92697-2575, USA
[b] National Fuel Cell Research Center, University of California, Irvine, CA 92697-3550, USA

HIGHLIGHTS

- We explore inter-diffusion in composite SOFC electrodes as a durability issue.
- Composite SSC/LSGM cathodes were synthesized at varying constituent weight ratios.
- System degradation was evaluated via electrochemical testing and TEM microanalysis.
- Degradation was correlated with microstructure-dependent cation inter-diffusion.
- TEM/EDS analysis is critical to understanding mechanisms and kinetics of evolution.

GRAPHICAL ABSTRACT

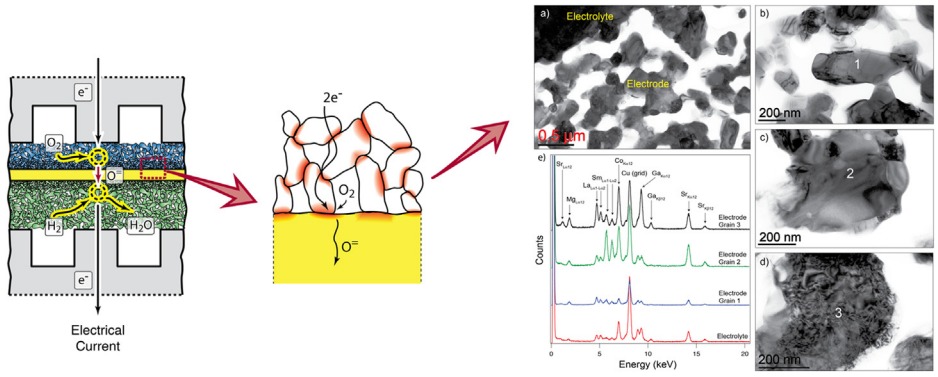

ARTICLE INFO

Article history:
Received 6 December 2012
Received in revised form
2 April 2013
Accepted 10 April 2013
Available online 25 April 2013

Keywords:
Solid oxide fuel cells
Cathodes
Inter-diffusion
Polarization
Electrode degradation

ABSTRACT

Composites of $Sm_{0.5}Sr_{0.5}CoO_{3-\delta}$ (SSC), a good electronic conductor, and $La_{0.8}Sr_{0.2}Ga_{0.8}Mg_{0.2}O_{3-\delta}$ (LSGM), a good ionic conductor, have been evaluated as cathode systems for La-gallate electrolyte based SOFC systems via microstructural analysis and electrochemical testing. SSC and LSGM composite cathode half-cells were fabricated with varying phase fraction ratios. X-ray diffraction and transmission electron microscopy studies show that these electrode and electrolyte materials will inter-diffuse with long-term exposure in service environments. Within an electrode, inter-diffusion occurs between SSC and LSGM particles of varying initial particle sizes, resulting in heterogeneity in the local cation ratios. Of the SSC/LSGM weight ratios analyzed (pure SSC, 80:20, 70:30, and 50:50), the 80:20 ratio was identified to possess the lowest resistance, according to AC impedance results. The microstructural basis of this finding, and implications for optimal materials design, are discussed.

1. Introduction

Solid oxide fuel cells (SOFCs) are energy conversion devices that have gained significant international interest for efficient distributed power generation, due to their fuel and materials flexibility. Their high operation temperature (500 °C–1000 °C) enables the use of a number of carbon-based fuels for electrical energy production, a clear advantage over low temperature polymer electrolyte fuel cells. Methane, propane, butane and coal-derived syngas can either be catalyzed or steam reformed directly in the anode (depending on the materials used) with high CO and sulfur tolerance. In addition, the improved kinetics associated with the high operation temperature allows the use of a diverse array of

* Corresponding author. Chemical Engineering and Materials Science, University of California, Irvine, CA 92697-2575, USA. Tel.: +1 949 824 3858; fax: +1 949 824 2541.
E-mail address: mumm@uci.edu (D.R. Mumm).

0378-7753/$ – see front matter © 2013 Elsevier B.V. All rights reserved.
http://dx.doi.org/10.1016/j.jpowsour.2013.04.046

electrode and electrolyte materials, avoiding the use of expensive catalysts (such as platinum) and reducing the cost per kW for electrical power production. Although SOFCs are bordering on widespread commercial viability, durability issues remain to be a barrier. In order to reach the durability target of <4% degradation per 1000 h for 5000 h system lifetimes (SECA guidelines for coal-based systems), efforts in optimizing performance and durability emerge as a major focus in SOFC research.

Attempts at improving SOFC durability result in an overall effort to engineer the cathode microstructure and explore alternative materials that enable a decrease in operating temperature [1]. Exploration of porous composite electrodes has demonstrated improved performance in two ways. First, mixing the electrode and electrolyte constituents within the electrode reduces the thermal expansion mismatch between the electrode and electrolyte components, avoiding failure due to thermal stresses. Second, composite electrodes have been demonstrated to improve electrode performance (specifically the cathode) due to an increase in the volumetric density of active triple phase boundary sites (interface between the electrode, electrolyte materials and the pores) [2–5]. This results in lower electrode resistance and over-potential loss, which benefits efforts to lower the operating temperature. Mixed ionic and electronic conductors (MIECs) have been explored as possible cathode materials for lower temperature operation. Unlike the purely electronically conducting materials, such as $La_xSr_{1-x}MnO_{3-\delta}$ (LSM), MIEC's demonstrate the ability to conduct both electrons and oxygen ions. These materials include the strontium doped ferrites and cobaltites, which have highly disordered, distorted crystal structures that enable bulk vacancy transport. The electronic conduction is attributed to the multi-valent states of Fe and Co in these materials. In order to utilize these materials, a compatible electrolyte is needed.

The development of new cathode/electrolyte systems has inspired much work on compatibility studies of materials [6–9]. As the scientific community moves toward developing new materials that have been heavily doped by aliovalient cations (such as the MIEC's), ensuring that these materials form functional interfaces is of great importance. This is especially true given that work on analyzing degradation of the cathode–electrolyte interface in SOFC systems comprising yttria-stabilized zirconia (YSZ) electrolytes with LSM cathodes (previously considered to be stable) produced evidence of cationic diffusion during electrode polarization [10]. Although studies of materials compatibility show stable, non-reacting interfaces with simple high temperature exposure, under the influence of both a potential and extended thermal exposure cation inter-diffusion may still pose a threat to the performance and durability of the fuel cell. In considering degradation mechanisms, there are two types of interactions that may take place when the electrode/electrolyte system undergoes thermal treatment. The bounding phases can thermo-chemically react to form a new phase that possesses its own space group and lattice parameter. Such interaction is seen when $La_xSr_{1-x}Co_yFe_{1-y}O_{3-\delta}$ (LSCF) reacts with YSZ to form $La_2Zr_2O_7$, a resistive pyrchlore phase [6]. Similarly, LSM and YSZ will also react at elevated temperatures (>1200 °C) to form pyrochlore phases. Using the system at lower temperatures where the reaction will not occur bypasses the reactivity problem.

The second interaction, not as heavily explored, is the inter-diffusion of the cation species (without new phase formation). This occurs when atoms from one material diffuse into the lattice of the second, to settle at a lattice or interstitial point of the second material. The effect of inter-diffusion is a change in defect chemistry in the regions around the interface of the bounding phases, causing a time-dependent variation in the electrochemical behavior of the system. Inter-diffusion has been shown to occur between various lanthanide material sets such as LSCF and $La_xSr_{1-x}Ga_yMg_{1-y}O_{3-\delta}$ (LSGM) [7], $La_xSr_{1-x}CoO_{3-\delta}$ (LSC) and LSGM [8], and $Pr_xSr_{1-x}Co_yMn_{1-y}O_{3-\delta}$ (PSCM) or $Pr_xSr_{1-x}Co_yFe_{1-y}O_{3-\delta}$ (PSCF) and LSGM [9]. Unlike the first kind of interaction discussed, inter-diffusion is a process that occurs at all temperatures. Consistent with the theory of diffusion, if rapid diffusion is to occur at 900 °C, then it is likely to occur at 700 °C but at a substantially slower rate. In the study of compatibility between constituent materials for SOFCs, inter-diffusion problems can be easily overlooked, compared to the more obvious phase formation reactions. A study by Wang et al. of the compositing of LSGMC with strontium doped samarium cobaltite (SSC) electrode material concluded that the two materials are compatible, based on the absence of new phases in the XRD spectra [11]. Evidence contrary to their findings will be revealed in this manuscript.

This manuscript explores the inter-diffusion problems of the lanthanum gallate electrolyte and strontium doped samarium cobaltite, both of which have been deemed promising materials for low temperature solid oxide materials [11–13]. $LaGaO_3$ doped with strontium in the A-site and magnesium in the B-site (to form $La_{1-x}Sr_xGa_{1-x}Mg_xO_{3-\delta}$) is a suitable electrolyte material for low temperature operation due to its high ionic conductivity and low thermal expansion. $Sm_{1-x}Sr_xCoO_{3-\delta}$ is a mixed ionic and electronic conductor with conductivity ranging over 1000 S cm^{-1} at temperatures between 200 °C and 800 °C. Their high conductivity render these materials ideal for low temperature operations. With the thermal expansion coefficient as high as 22.8×10^{-6} K^{-1} [14], SSC is best used as a cathode constituent as a composite with LSGM or other electrolyte material [11–13,15]. This manuscript will show that although these two materials demonstrate favorable thermal and electrochemical attributes, they undergo cationic inter-diffusion when mixed and sintered. This renders the compositing of SSC and LSGM an unlikely choice for stable, degradation resistant electrode systems. Electrochemical manifestation of the observed inter-diffusion will be discussed.

2. Experimental procedures

The compatibility of $Sm_{0.5}Sr_{0.5}CoO_{3-\delta}$ (SSC) and $La_{0.8}Sr_{0.2}Ga_{0.8}Mg_{0.2}O_{3-\delta}$ (LSGM) was studied by analyzing pellets of the individual compounds and of the composite mixtures. Both LSGM and SSC were synthesized by the glycine nitrate processing (GNP) route [16]. For SSC, samarium nitrate hexahydrate, strontium nitrate, and cobalt nitrate hexahydrate precursors were dissolved in deionized water at the prescribed stoichiometric ratios. Glycine was added into the mixture after the dissolution of the metal nitrates. The slurry was heated with a hotplate and allowed to form a gel until a self-sustaining combustion reaction occurs, with the resulting ash as the product. The powder was calcined at 1190 °C. A similar method was used to synthesize LSGM using lanthanum nitrate hexahydrate, strontium nitrate, gallium nitrate hydrate, and magnesium nitrate hexahydrate as precursors. The resultant powder was calcined at 1450 °C in order to obtain the perovskite phase. A third composition was synthesized which consists of all cations (La, Sr, Ga, Mg, Sm, and Co) with stoichiometric ratios summarized in Table 1.

Table 1
Composition (atomic percent) of elements targeted in the synthesis of LSSGMC.

Crystallographic position	Element	Stoichiometry
A site	Lanthanum	0.40
	Strontium	0.35
	Samarium	0.25
B site	Gallium	0.40
	Magnesium	0.10
	Cobalt	0.50

These ratios were calculated based on the resulting stoichiometry of a 50:50 SSC/LSGM weight % composition. The composite powders of SSC and LSGM, mixed at ratios of 80:20, 70:30 and 50:50 weight % (94, 89 and 79 volume % SSC, respectively), were prepared by ball-milling for 24 h.

2.1. X-ray diffraction and microanalysis

Pellets of all the synthesized compositions and the composite powder mixtures were made using a uni-axial press and a 13 mm die, pressed at 67 MPa for 5 min followed by cold isostatic pressing at 379 MPa for 5 min. The firing temperature was 1000 °C. In addition to the pure SSC and LSGM pellets, four composite pellets of 50:50 weight ratio of SSC:LSGM were made and heat treated at 700 °C, 800 °C, 900 °C, and 1000 °C for 2 h. X-ray diffraction (XRD) scans (using an Seimens D5000 system) of all the pellets were taken. To confirm that cationic diffusion took place and resulted in a complete re-organization of the crystal structure and lattice parameter, the XRD pattern of the compound consisting of La, Sm, Sr, Ga, Mg, and Co (LSSGMC) was compare to that of the composite and heat treated pellets.

2.2. Specimen configuration and electrochemical testing

AC impedance (using a four-point connection) was used for electrochemical characterization on symmetric half-cells (Fig. 1). The electrolytes were made using a uni-axial press (33 mm die, 10.4 MPa applied pressure) followed by cold isostatic pressing (379 MPa) to form pellets that are ~2 mm thick and 20 mm in diameter after sintering. Both surfaces of the pellets were polished to make cross sections parallel. The fabrication of symmetric half-cells starts with ball milling mixtures of SSC and LSGM for 24 h in ethanol. The composite powders are screen-printed onto the electrolyte pellets using a Heraeus Vehicle 600 binder. The cells are then co-fired at 1000 °C for 1 h. The specimens are configured with screen-printed circular working and counter electrodes of 0.88 cm^2 areas (Fig. 1). Pt paste (BASF) was brush-painted on top of the cathode layer and co-fired at 1000 °C for 1 h. Platinum gauze (Alfa Aesar, 52 mesh woven from 0.1 mm diameter wire, 99.9% Pt) was used to make the electrical connection. AC impedance measurements at open circuit potential (OCP) were taken using a Solartron 1287 potentiostat coupled with a Solartron 1260 impedance analyzer. Data were collected using Corware and Zplot software tools, over the temperature range of 500 °C–800 °C. A total of 5 cathodes were fabricated and tested: pure SSC, LSSGMC, and three SSC/LSGM composite cathodes of mixing ratio 80:20, 70:30 and 50:50 weight %.

2.3. TEM analysis

Subsequent to electrochemical testing of the 50:50 SSC:LSGM ratio half-cell, transmission electron microscopy (TEM) was used to analyze the microstructure, composition, and crystallographic information of inter-diffused electrode grains. The half-cell was fractured to expose the cross-section. The electrode pores were infiltrated with a metallurgical grade of epoxy (Epothin, Buehler). The surface of the epoxy filled sample was polished using diamond lapping films (South Bay Technology). The TEM specimen was extracted from the epoxy-mounted sample using a FIB/SEM (FEI Quanta with Omni Probe). For TEM, the Philips CM20 was used. Energy dispersive spectroscopy (EDS) and electron diffraction patterns were obtained and analyzed for the crystallographic parameters of the new phases and altered chemistry domains formed by inter-diffusion.

3. Results

3.1. X-ray diffraction analysis

XRD spectra of the SSC, LSGM and the four composite pellets of 50:50 ratio that were sintered at 700 °C, 800 °C, 900 °C and 1000 °C are shown in Fig. 2. The diffraction pattern for 700 °C shows two sets of peaks that correspond to SSC and LSGM. The patterns of pellets sintered at 800 °C, 900 °C, 950 °C, and 1000 °C show a merging of the two sets of peaks. Fig. 3 shows XRD patterns of SSC, LSGM and the composite pellet sintered at 1000 °C between the diffraction angle 2θ values of 31° and 35°. Extracted from the XRD spectra in Fig. 2, Fig. 4 shows the growth of the $LaSrGa_3O_7$ peak located between 29° and 31°. Fig. 5 shows an XRD pattern of a synthesized LSSGMC material, compared to that of the 50:50 ratio SSC/LSGM composite pellet sintered at 1000 °C.

3.2. Electrochemical analysis

AC impedance curves that resulted from the 4-point probe measurements are shown in Fig. 6. A single R-CPE circuit with a serial resistance equivalent resistance (Fig. 7) was used to fit the curves. From these fits the polarization resistance (R_p) was extracted. Table 2 summarizes the R_p values normalized for electrolyte thickness. Fig. 8a plots the R_p values with respect to weight% SSC. Plots of $\ln(R_p)$ versus $1/T^*k$ (where T is temperature in kelvin

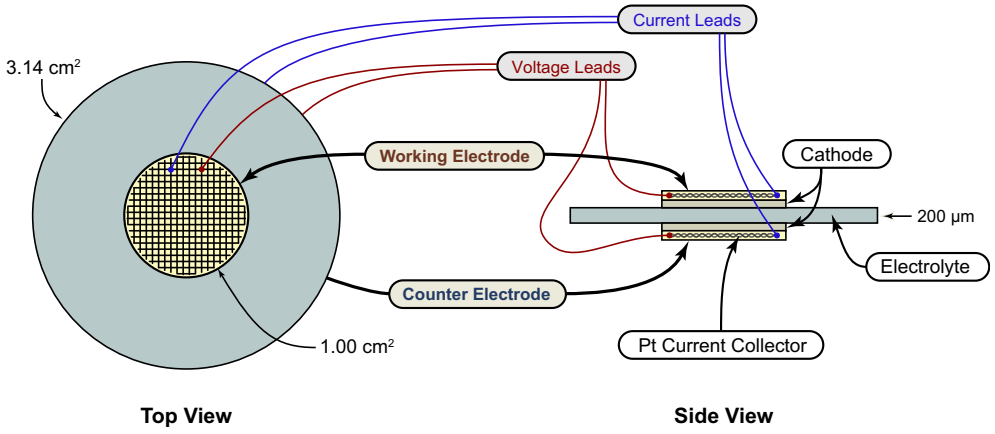

Fig. 1. Schematic diagram of the 4-electrode configuration used for AC impedance measurements (not drawn to scale).

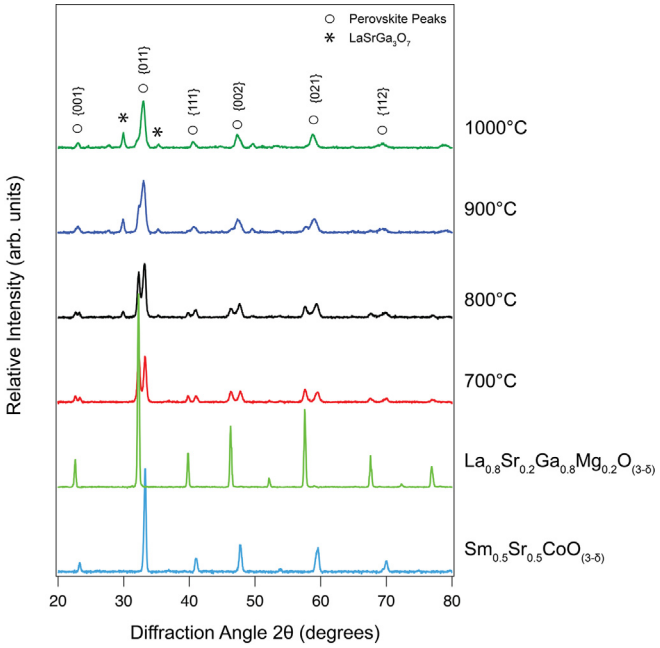

Fig. 2. X-ray diffraction pattern of pellets of pure SSC (sintered at 1000 °C), pure LSGM (sintered at 1450 °C) and composites sintered at 700 °C, 800 °C, 900 °C, 950 °C, and 1000 °C. All patterns were collected at room temperature.

and k is Boltzmann's constant), show a linear relationship indicating that the kinetics of the process is activation controlled (Fig. 8b). Following the Arrhenius relationship of $R_p = R_0\exp(E_a/kT)$, the activation energy, E_a, values can be calculated using the slope of the linear curves.

3.3. TEM analysis

Micrographs of TEM lamella samples, extracted from the post-test 50:50 weight ratio sample, are shown in Fig. 9. Fig. 9a shows an overview of the electrolyte and porous electrode cross-section. The electrolyte and electrode portions of the lamella can be seen in the overview in Fig. 9a. EDS spectra were collected on various electrode grains by tuning the condensed beam to a spot size that ensures that the condensed beam was isolated within the individual grains, avoiding beam interaction with neighboring grains. A count time of 4 min was used for all grains analyzed. The EDS spectra in Fig. 9e correspond to the micrographs of electrode grains in Fig. 9b–d. Also included in Fig. 9e is the EDS spectrum taken from an electrolyte region close to the electrode.

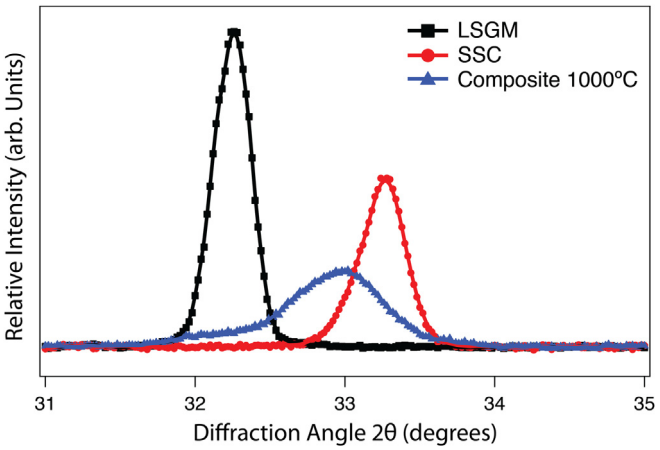

Fig. 3. A comparison of X-ray peaks between diffraction angle 2θ values of 31° and 34° of spectra taken from pellets of pure SSC sintered at 1000 °C, pure LSGM sintered at 1450 °C, and a composite pellet sintered at 1000 °C. All patterns were collected at room temperature.

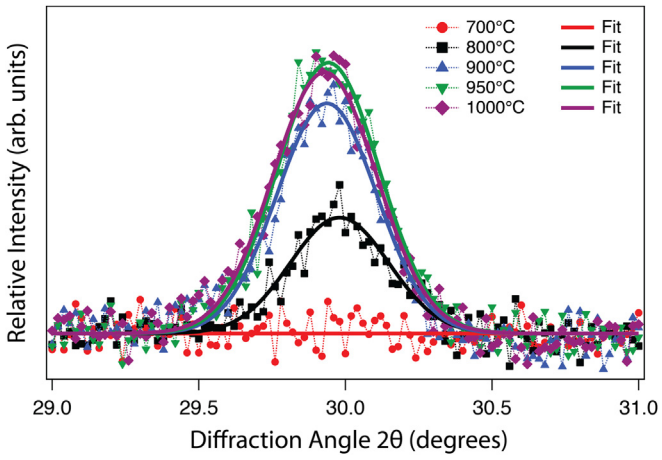

Fig. 4. X-ray diffraction patterns of SSC-LSGM composite pellets (50:50 ratio) sintered at 700 °C, 800 °C, 900 °C, 950 °C and 1000 °C, evaluated at diffraction angle 2θ values between 29° and 31°.

4. Discussion

Confirmed by XRD, the onset of inter-diffusion occurred at between 700 °C and 800 °C. The emergence of $LaSrGa_3O_7$ peaks was observed in the XRD spectra corresponding to sintering temperatures above 800 °C. Complete inter-diffusion of the screen-printed porous electrode after electrochemical testing was not observed, as shown by the differences in performance of all the mixing ratios, as well as their difference when compared to the LSSGMC cathode. The electrochemical tests of the various mixing ratios identified the 80:20 ratio to be highest in performance (lowest polarization resistance).

4.1. Inter-diffusion discussed in literature

The presence of cobalt in materials has been shown to cause instability in composite systems. It was suggested that Co diffuses more than other elements, confirmed by other's study of composite

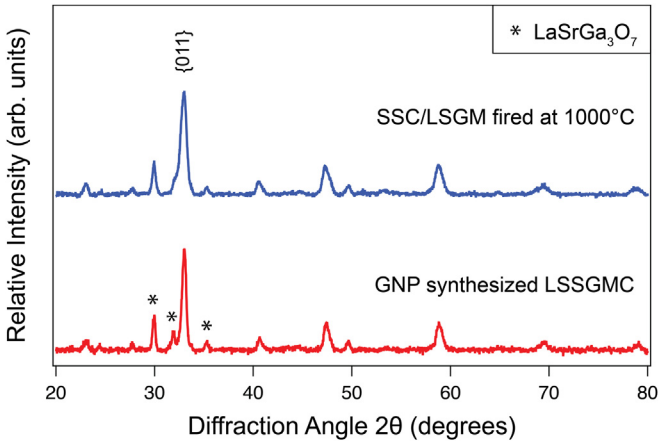

Fig. 5. X-ray diffraction patterns of a LSSGMC pellet synthesized by GNP, and sintered at 1000 °C, and a composite pellet also sintered at 1000 °C.

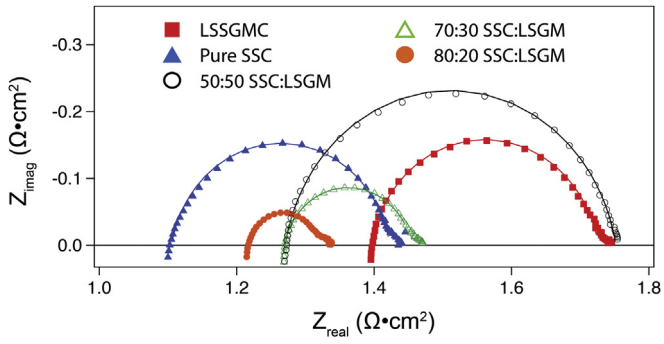

Fig. 6. AC impedance curves collected at OCP at 750 °C for all compositions.

systems [8,9,17]. Huang and Goodenough et al. [8] showed that inter-diffusion occurred in the compositing of LSGM and LSC in which Ga atoms diffuse into the LSC lattice and Co diffuse into the LSGM lattice, but the compositing of LSGM and LSM showed no such inter-diffusion problem. Kostogloudis et al. commented on the formation of the $LaSrGa_3O_7$ peaks from inter-diffusion in their comparison of the stability of $La_{0.9}Sr_{0.1}Ga_{0.8}Mg_{0.2}O_{3-\delta}$ with $Pr_{0.8}Sr_{0.2}Co_{0.2}Mn_{0.8}O_{3-\delta}$ and $Pr_{0.8}Sr_{0.2}Co_{0.2}Fe_{0.8}O_{3-\delta}$ and $La_{0.8}Sr_{0.2}Ga_{0.9}Mg_{0.1}O_{3-\delta}$ with $Pr_{0.8}Sr_{0.2}Co_{0.3}Mn_{0.7}O_{3-\delta}$ and $Pr_{0.75}Sr_{0.2}Co_{0.2}Mn_{0.8}O_{3-\delta}$ at 1300 °C. Their observation is that transition metal diffusion into the LSGM lattice enhances the stability of the Sr cation, resulting in the reduction of $LaSrGa_3O_7$ peaks in XRD data [9]. Thus, the diffusion of Co from PSCM and PSCF helped to stabilize the Sr in the LSGM lattice. In the case of the current experiment, the opposite was observed. The $LaSrGa_3O_7$ peaks increased with increasing sintering temperature. It was also mentioned by Kostogloudis et al. that 20 mol% of Sr atoms in the LSGM is the upper limit of the amount of Sr doping possible in the matrix. Diffusion of additional cations into the A-site may result in the depletion of Sr in the perovskite, contributing to formation of the $LaSrGa_3O_7$ phase. In addition, Kharton's analysis of TEC with respect to Co contents in materials concluded that the defect chemistries that allow these materials to be highly conducting also increase the TEC and ionic conductivity by lowering the activation barrier for cationic mobility [17]. Summaries of TEC show that cobaltites possess the highest TEC. Since SSC has a TEC of $\sim 22.8 \times 10^{-6}\ K^{-1}$, it is not surprising that it shows a great amount of instability when interfaced with other materials.

4.2. XRD and microstructure analysis

Figs. 2–5 are clear indications of cationic inter-diffusion between the SSC and LSGM phase. From Fig. 2, it is apparent that as the composite pellet is heat treated from 800 °C to 1000 °C, a new perovskite phase forms. Complete inter-diffusion is accomplished at 1000 °C in which the peaks corresponding to the new perovskite phase possess a different set of lattice parameters than that of the pure SSC and LSGM phases. This is shown in the emergence of the {011} peak of the inter-diffused phase shown in Fig. 3. Fig. 2 also shows the gradual growth in intensity of the peak at 30° for SSC and

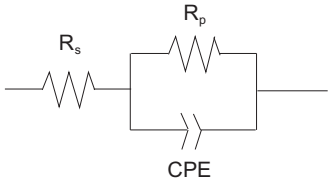

Fig. 7. Equivalent circuit showing solution resistance (R_s), polarization resistance (R_p) and a pseudo-capacitance (CPE) used to fit the impedance curves shown in Fig. 6.

Table 2
R_p (Ωcm^2) values resulting from fitting AC impedance results to the equivalent circuit shown in Fig. 7, for all samples. The trend for all temperatures shown indicates that the 80:20 composition possesses the lowest polarization resistance, and the pure SSC, the highest.

Composition	Test temperature						
	500 °C	550 °C	600 °C	650 °C	700 °C	750 °C	800 °C
LSSGMC	583.11	145.45	46.00	21.54	9.24	2.96	1.30
5:5	1373.06	339.07	94.69	30.05	7.80	4.52	2.14
7:3	565.58	126.55	32.65	10.09	10.91	1.65	0.87
8:2	168.76	42.50	12.29	5.27	3.75	1.02	0.52
Pure SSC	1907.85	399.63	94.33	26.08	2.09	3.37	1.34

LSGMC composite pellets. At 800 °C, these peaks begin to grow such that at 1000 °C, the intensity is highest. These peaks correspond to the $LaSrGa_3O_7$ phase that resulted from inter-diffusion. The growth of the $LaSrGa_3O_7$ peak with temperature, shown in Fig. 4, suggests that $LaSrGa_3O_7$ formation is dependent on the extent of inter-diffusion. At 1000 °C, corresponding to complete inter-diffusion, the $LaSrGa_3O_7$ peak intensity is highest. Fig. 5 compares the XRD patterns acquired from the composite pellet sintered at 1000 °C for 2 h and the GNP synthesized LSSGMC pellet. The peak overlap between the two spectra is evidence that a complete mixture of cations from the starting materials is achieved after the temperature treatment. The additional peaks that are not assignable to the perovskite phase (indicated by the open circle symbols) belong to $LaSrGa_3O_7$ and are also present in both patterns. These results support the observation that cation diffusion has lead

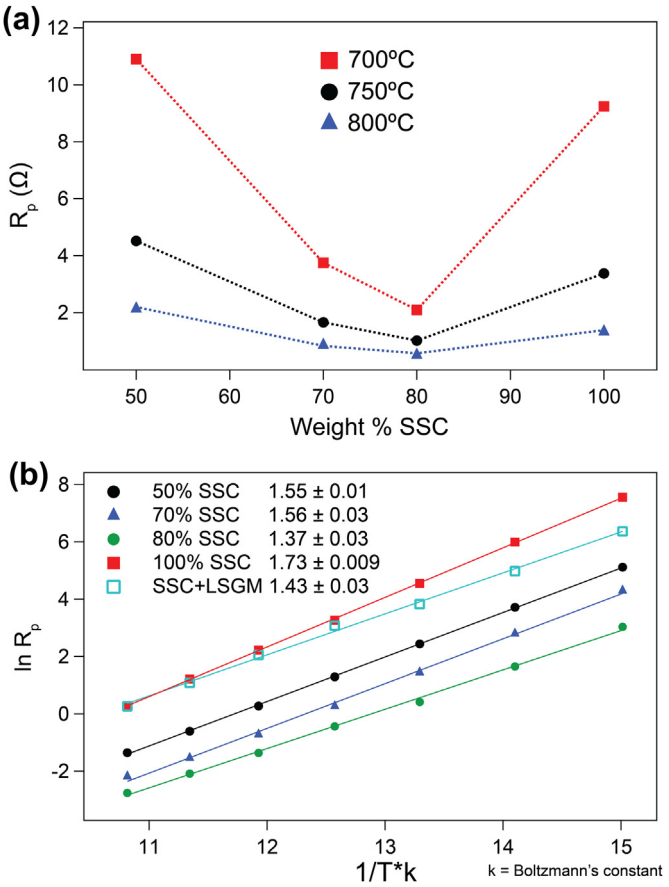

Fig. 8. Plots showing (a) R_p values vs. weight% SSC and (b) the Arrhenius relationship between R_p and temperature, with calculated activation energy (eV) values.

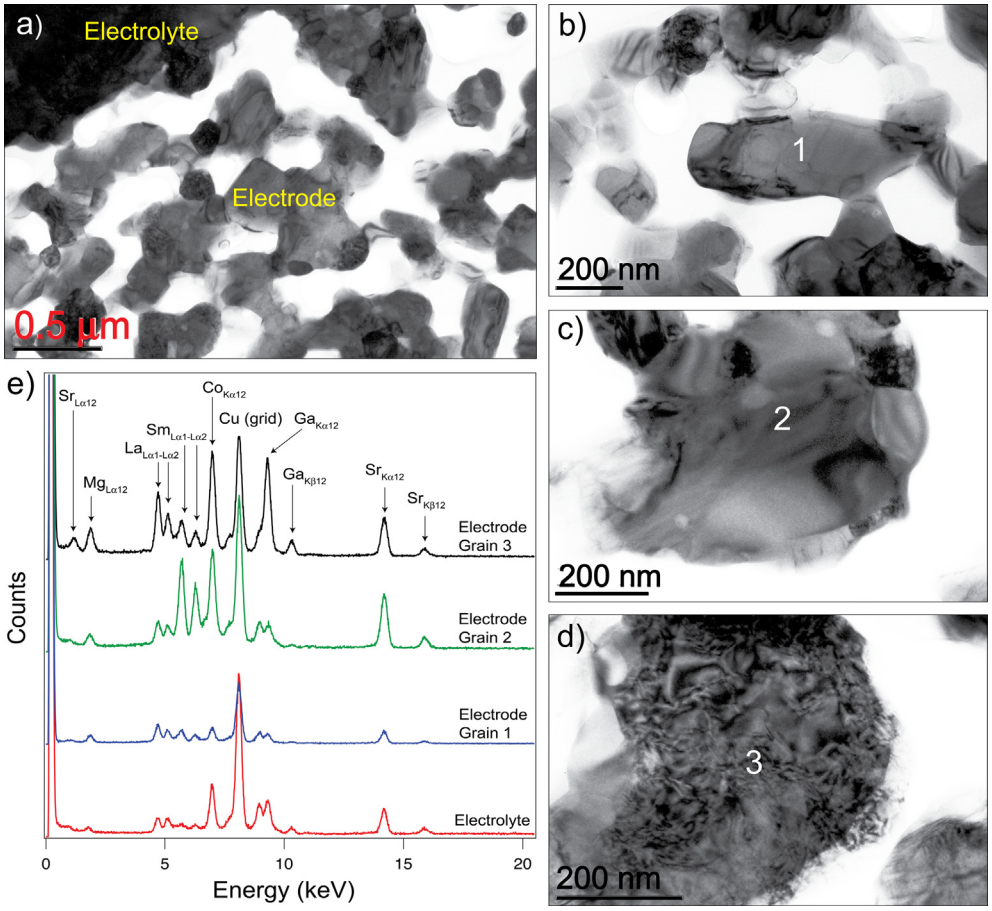

Fig. 9. TEM results showing (a) an overview of the TEM lamella, (b)–(d) electrode grains analyzed by EDS, and the resulting EDS spectra shown in (e). All grains analyzed are extracted from the 50:50 post-test specimen.

to complete mixing similar to the kind that resulted from GNP synthesis using all the metal nitrates as precursors.

EDS analysis of the grains within the TEM lamella also provides clear evidence that inter-diffusion between the SSC and LSGM particles within the electrode results in an electrode of heterogeneous chemistry. The EDS spectra shown in Fig. 9e (of the inter-diffused grains examined in Fig. 9b–d) indicates the presence of all constituent cations in all of the electrode grains analyzed, as well as in an electrolyte area near the electrode. Qualitative comparison of the peak heights of the electrode grains shows that cations are present in varying amounts. Unlike the interface of the LSGM/SSC pellets (in which interface areas are large, enabling enhanced inter-diffusion with diffusion rates that can be characterized as a uniform average), the interface areas in a representative electrode microstructure differ depending on the size and shape of the SSC and LSGM grains in their initial, non-diffused state. Since diffusion is dependent on a concentration gradient, the varying grain sizes result in localized diffusion profiles, which explains the differences in cation ratios among the electrode grains in Fig. 9e. The EDS spectrum correlated with the electrolyte region appears to be rich in cobalt, which supports the discussion in Section 4.1 that cobalt diffuses most readily. Comparing the relative intensities of the cations present for the electrode grains show evidence that inter-diffusion may occur to varying extents, depending on the interfacial area of neighboring grains. The higher apparent content of samarium, cobalt and strontium compared to lanthanum, magnesium and gallium in the examined electrode grain 2 suggests that inter-diffusion has occurred between a SSC grain and a measurably smaller contacting LSGM grain. The opposite is observed for electrode grain 3 in which La, Mg, and Ga intensities appear to be higher than that observed for Sr and Sm cations, suggesting that inter-diffusion took place between a larger LSGM grain and a smaller SSC grain. Due to localized differences in cation concentration related to the size, shape and interfacial area of the neighboring SSC and LSGM particles, electrodes of SSC and LSGM mixtures will have time-dependent heterogeneous cation concentrations, and associated variations in electrochemical properties.

4.3. Electrochemical analysis

Table 2 and Fig. 8 summarize the AC impedance results of the different ratios of SSC and LSGM cathodes. The R_p values collected for all temperatures and summarized in Table 2 indicate that the cathode performance varies with different phase fraction ratios. The LSSGMC cathode also shows performance that is different, which indicates that complete inter-diffusion may not have been achieved in the other cathode systems. The heat treatment of the porous cathodes and the composite pellets are similar in that both have been heat treated for 2 h. For the composite pellets, heat treatment for 2 h and 1000 °C resulted in uniform inter-diffusion. The same heat treatment for composite cathodes did not yield the same result. The difference in polarization resistance values for the LSSGMC and the 50:50 ratio cathode may be due to localized variance in cation concentration, as explained in Section 4.2.

From Fig. 8a, it is evident that the 80:20 mixing ratio possess the lowest polarization resistance and that the pure SSC cathode is lowest in performance. With evidence of incomplete inter-diffusion, it is likely that the LSGM and SSC maintain their initial function as ionic conductor and MIEC, respectively. Therefore, the 80:20 composition may represent a good compromise between ionic and electronic contributions. The activation energy values shown in Fig. 8b also points to the 80:20 composition as the more efficient cathode (1.37 eV compared to 1.73 eV for pure SSC and 1.43 eV for LSSGMC).

5. Summary and conclusions

The compatibility of SSC and LSGM as constituents of composite SOFC cathodes was studied. This set of data show the electrochemical manifestation of inter-diffusion in cathode electrodes and demonstrates that these interfaces are crucial to the performance. It is clear that with inter-diffusion, a layer forms at the phase boundaries with chemistry and structure distinct from the SSC and LSGM electrode constituents. At temperatures above 800 °C, inter-diffusion was accompanied by the formation of a $LaSrGa_3O_7$ second phase, the prevalence of which increases with increasing sintering temperature. In a composite electrode, uniform distribution of cation concentration was not achieved over the test periods studied. The extent of inter-diffusion varies depending on the size of neighboring grains (i.e. the evolution of the system is microstructure-dependent). Due to the temperatures at which inter-diffusion occurs being consistent with the intended SOFC service environments, SSC and LSGM are incompatible compositing couples. As such, composites of other materials that show a tendency for inter-diffusion may demonstrate similar behavior in that the performance may be compromised.

Acknowledgments

The authors acknowledge the Laboratory for Electron and X-ray Instrumentation (LEXI) at the University of California, Irvine. This material is based upon work supported by the National Science Foundation under Grant No. 0645812. Any opinions, findings, and conclusions or recommendations expressed in this material are those of the authors and do not necessarily reflect the views of the National Science Foundation.

References

[1] R. Knibbe, A. Hauch, J. Hjelm, S.D. Ebbesen, M. Mogensen, Green 1 (2011) 141–169.
[2] A.T. Duong, D.R. Mumm, J. Electrochem. Soc. 159 (2012) B40–B53.
[3] T. Kenjo, M. Nishiya, Solid State Ionics 57 (1992) 295–302.
[4] M. Ostergard, C. Clausen, C. Bagger, M. Mogensen, Electrochim. Acta 40 (1995) 1971–1981.
[5] M. Juhl, S. Primdahl, C. Manon, M. Mogensen, J. Power Sources 61 (1996) 173–181.
[6] L. Kindermann, D. Das, H. Nickel, K. Hilpert, Solid State Ionics 89 (1996) 215–220.
[7] N. Sakai, T. Horita, K. Yamaji, M. Brito, H. Yokokawa, J. Electrochem. Soc. 153 (2006) A621–A625.
[8] K. Huang, M. Feng, J. Goodenough, M. Schmerling, J. Electrochem. Soc. 143 (1996) 3630–3636.
[9] G.C. Kostogloudis, C. Ftikos, A. Ahmad-Khanlou, A. Naoumidis, D. Stover, Solid State Ionics 134 (2000) 127–138.
[10] M. Backhaus-Ricoult, Solid State Sci. 10 (2008) 670–688.
[11] S.Z. Wang, Y.M. Zou, Electrochem. Commun. 8 (2006) 927–931.
[12] S.Z. Wang, H. Zhong, Y.M. Zou, J. Power Sources 161 (2006) 1154–1160.
[13] S.Z. Wang, L.L. Wu, Y. Liang, J. Power Sources 166 (2007) 22–29.
[14] S. Yang, T.M. He, Q. He, J. Alloys Compd. 450 (2008) 400–404.
[15] C.R. Xia, W. Rauch, F.L. Chen, M.L. Liu, Solid State Ionics 149 (2002) 11–19.
[16] L.A. Chick, L.R. Pederson, G.D. Maupin, J.L. Bates, L.E. Thomas, G.J. Exarhos, Mater. Lett. 10 (1990) 6–12.
[17] V.V. Kharton, A.A. Yaremchenko, E.N. Naumovich, J. Solid State Electrochem. 3 (1999) 303–326.